

IMF FROM INFRARED PHOTOMETRY OF YOUNG STELLAR CLUSTERS IN TAURUS-AURIGA AND ORION

Luis Salas and Irene Cruz-González

Instituto de Astronomía, Universidad Nacional Autónoma de México, Mexico

Received 2009 June 8; accepted 2009 September 16

RESUMEN

Se aplicó el método de vectores principales de disco y extinción a los datos fotométricos en el cercano infrarrojo de los cúmulos estelares jóvenes de las regiones Tauro-Auriga y Orión. Bajo la suposición de que la edad del cúmulo está representada por la mediana de la distribución de edades se obtiene una estimación de las masas estelares individuales. La función inicial de masa (FIM) obtenida para estos cúmulos exhibe una gran similitud con la obtenida por métodos espectroscópicos y fotométricos y puede constituir una representación robusta de la FIM. El método permite encontrar la contribución por extinción y disco para cada estrella. La distribución global de la extinción para el cúmulo de Orión se compara bien con resultados previos. Se encuentra que la frecuencia de estrellas T Tauri con disco es del orden de 50%.

ABSTRACT

We applied the extinction-disk-principal vectors approach to near infrared photometric data of the Taurus-Auriga region and Orion Nebula young stellar clusters. By assuming that the cluster age is represented by the median value of the age distribution we are able to derive the distribution of stellar masses. We showed that the resulting initial mass function (IMF) for these two young stellar clusters compares remarkably well and might be a robust representation of the IMF obtained by spectroscopic or photometric methods. The method also yields the extinction and disk contribution for each star. The overall extinction distribution for the Orion cluster is analyzed and compares well with previous work. The frequency of T Tauri stars with disks is about 50%.

Key Words: stars: formation — stars: fundamental parameters — stars: low-mass, brown dwarfs — stars: pre-main sequence

1. INTRODUCTION

Masses of pre-main sequence (PMS) objects are quite difficult to determine, and the only direct way to assess them is through the analysis of their dynamical parameters. Following Cohen & Kuhn (1979) locating objects in a temperature-luminosity H-R diagram along with evolutionary models yields masses. Since stellar temperature is estimated from colors, and these are affected by circumstellar disks, PMS temperatures are best estimated spectroscopically (e.g., Luhman et al. 2005). But PMS objects are usually faint and found in dusty environments and obtaining their spectra becomes quite difficult. This has led many authors to explore the initial mass function (IMF) of young stellar clusters in the in-

frared, via the luminosity function in the K -band (e.g., Muench et al. 2002), assuming that it reproduces the true IMF of a cluster. Color-color (CC) and color-magnitude (CM) near-infrared diagrams of young stellar clusters show that intrinsic near-infrared colors of young stars are affected both by interstellar extinction and by disk excess emission (Lada & Adams 1992; Hillenbrand et al. 1992; Meyer, Calvet, & Hillenbrand 1997; Hillenbrand & Carpenter 2000).

López-Chico & Salas (2007, hereafter LS07), showed that masses of T Tauri stars can be obtained using JHK photometry and both CC and CM diagrams. This is the result of the analysis of two principal vectors, one produced by the disk excess, \vec{D}

and the other by interstellar extinction, \vec{X} , if stellar ages are known and a particular set of evolutionary tracks is assumed.

In this paper we continue the development of a new approach in determining masses of pre-main sequence stars from near-infrared photometry. Our goal is to strengthen the results reported previously in LS07. First, we refine the values of disk excess coefficients given in LS07 by showing that the method can be extended to the *I* and *L* filters, and that these coefficients scale well with wavelength. This analysis is presented in § 2. Second, we test whether the method can be used to extract the Initial Mass Function (IMF) of young stellar clusters from infrared photometric data alone. § 3 shows that if the age of a young cluster is known the distribution of stellar masses can be obtained from their *JHK* photometry and a set of PMS evolutionary tracks. As a proof of this statement we apply the method to the well studied Taurus-Auriga region and to the Orion Nebula Cluster. It is shown that the median age of the clusters produces an excellent agreement with previously known IMFs. These results are reported in §§ 4 and 5, while a summary of our results is presented in § 6.

2. METHOD DESCRIPTION

LS07 showed that masses of T Tauri stars can be obtained using their *JHK* photometry and their location in both CC and CM diagrams. This is the result of the analysis of two principal vectors, one produced by the disk contribution, \vec{D} , and the other by interstellar extinction, \vec{X} . LS07 show that the vector \vec{X} can be defined as the extinction vector corresponding to $A_V=10$ with components given in Rieke & Lebofsky (1985), while the vector \vec{D} is obtained via *J*, *H*, and *K* magnitudes obtained from D'Alessio et al. (2005) models of accretion disks irradiated by a central T Tauri star. These base vectors were thus given the following components in the CM (*K* vs. (*J* - *K*)) and CC ((*J* - *H*) vs. (*H* - *K*)) diagrams:

$$\begin{aligned} \widehat{D}_{\text{cm}} &= (1.014, -1.105); \widehat{X}_{\text{cm}} = (1.68, 1.16), \\ \widehat{D}_{\text{cc}} &= (0.767, 0.221); \widehat{X}_{\text{cc}} = (0.61, 1.07). \end{aligned} \quad (1)$$

The position of a particular star in these CC and CM diagrams becomes then a vector sum in each diagram that can be reduced to a closure relation plus the following set of linear equations:

$$\begin{aligned} J &= J_0 + \alpha x_J - \beta y_J, \\ H &= H_0 + \alpha x_H - \beta y_H, \\ K &= K_0 + \alpha x_K - \beta y_K, \end{aligned} \quad (2)$$

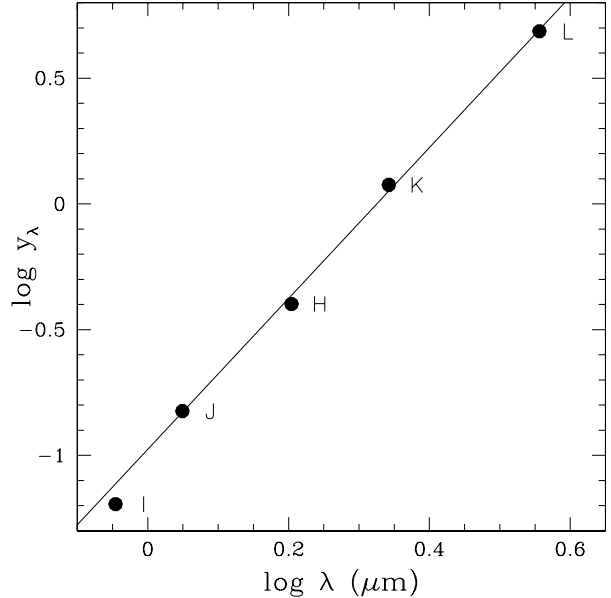


Fig. 1. Plot of $\log y_\lambda$ as a function of $\log \lambda$ shows that for IJHKL the data are well represented by a power-law of index=3, shown as a solid line.

where α and β represent the amount of extinction and infrared excess contributions to the individual magnitudes, x_λ and y_λ are the corresponding extinction and disk coefficients for each wavelength λ , and the zero sub-indices denote the intrinsic photospheric magnitudes. Values for x_λ and y_λ are obtained directly from the components of base vectors given in equation (1) and are presented in Table 1.

An advantage of presenting the equations as a set of linear equations is that it can be easily explored with any set of three photometric filters at a time, that is, we may use filters *IJK* or *JKL* instead of *JHK*, provided that the corresponding closure condition is fulfilled and that the excess colors behave as vectors. We found that this procedure is also feasible for filters *I* and *L* in addition to the *JHK* set, and so the numerical values of the y_λ coefficients for *I* and *L* are included in Table 1. We show in Figure 1 that the relation between $\log y_\lambda$ and $\log \lambda$ can be well represented by a power-law index equal to 3. This close relation gives us confidence to refine the y_λ values as given in the last column of Table 1, which are the values that we used in our analysis.

As is shown in LS07 stellar masses can be obtained from the solutions of the minimization of the quadratic error Err given by

$$\text{Err}^2 = \sum_{\lambda=1}^n \frac{(m_\lambda - m_\lambda^{\text{obs}})^2}{n}, \quad (3)$$

TABLE 1
COEFFICIENTS X_λ AND Y_λ FOR EXTINCTION
AND DISK CONTRIBUTIONS

Filter	x_λ^a	y_λ	y_λ^b
I	4.82	0.064	0.08
J	2.82	0.15 ^c	0.15
H	1.75	0.40 ^c	0.43
K	1.12	1.19 ^c	1.12
L	0.58	4.86	4.93

^aFrom Rieke & Lebofsky (1985).

^bUsing $y_\lambda \propto \lambda^3$.

^cFrom López-Chico & Salas (2007).

where m_λ^{obs} is the observed magnitude at each wavelength λ and m_λ is the magnitude that should be observed according to the model:

$$m_\lambda = m_\lambda^0(\text{mass, age}) + d + \alpha x_\lambda - \beta y_\lambda. \quad (4)$$

In equation (4) the stellar magnitude is the sum of the absolute magnitude for a certain mass and age, plus the distance modulus d to the object, plus the extinction correction and the infrared excess contribution from the circumstellar disk. The error is then minimized with respect to its four parameters: mass, age, α and β . This minimization procedure is a set of linear equations for α and β . To deal with mass and age we compute Err for each single mass and age taken from pre-main sequence evolutionary models. Then one seeks the minimum of Err consistent with the additional constraints $\alpha > 0$ and $\beta > 0$ obtained for each star. This method is called the extinction-disk principal vector, XDPV, method.

To test the XDPV method we will use only the PMS tracks from D’Antona & Mazzitelli (1997) and <http://www.mporzio.astro.it/~dantona/prems.html> that provide luminosities and temperatures for pre-main sequence stars in a wide low-mass range, from 0.017 to 3 M_\odot and ages from 10^4 to 10^8 yr. The use of other evolutionary tracks (e.g., Palla & Stahler 1999), has been discussed in LS07. These authors argue that these tracks are found to produce similar mass results within 20%. Luminosity and effective temperature of the evolutionary tracks are converted into absolute magnitudes using bolometric corrections and normal colors given in Kenyon & Hartmann (1995).

3. MASSES OF YOUNG STELLAR CLUSTER STARS

In LS07 we showed that if the masses of young stars are known, e.g. spectroscopically, the proposed XDPV method is a powerful tool to derive their ages or conversely, if the ages are known the masses can be extracted. However, both cannot be derived simultaneously. This is due, as pointed out in LS07, to the fact that the minimum of Err as a function of mass and age is a region that resembles a long and narrow canyon (c.f. their Figure 7) that spans a wide range in masses and ages, providing a continuum of possible solutions. It is then necessary to specify an age for the PMS object to determine its mass.

However, when dealing with a cluster of stars with similar ages, a representative age of the cluster may be used for all the individual members. Doing so requires a compromise age that would compensate the errors in mass by assuming too young an age for some objects with the errors derived from assuming an older age. The median age bisects the age histogram in equal parts, so that an equivalent number of members is either younger or older. Furthermore, the median is a robust indicator of the central tendency, its value is the same whether one uses the histogram of ages in linear or logarithmic values, and in general, is a better choice when we only have one number to specify a distribution. For these reasons, we have chosen to use the median age of each cluster.

We will show that this age selection gives consistent results for the resulting mass histograms of the well studied young stellar clusters of Taurus-Auriga and Orion, through the comparison of the IMF obtained by other authors using spectroscopic or photometric methods, and the IMF obtained applying our algorithm. We note that in the young stellar clusters studied here, the median age has a lower value than the mean, due to the fraction of younger stars in the tail of the distribution. For Taurus-Auriga we obtain $\log \text{median} = 5.8$ (0.63 Myr) and $\log \text{mean} = 5.95$ (0.89 Myr), while for Orion $\log \text{median} = 5.6$ (0.4 Myr) and $\log \text{mean} = 5.8$ (0.63 Myr), as is described in detail below. These values are significantly younger than what is commonly assumed as the age of the clusters. But this has to be so, because one usually refers to the epoch at which star formation began, which is the upper limit of the age distribution.

The method produces very good results as is shown below. Although it may seem a disadvantage to have to specify a cluster age, it is still far less information that the requirement of spectral types

in spectroscopic methods, or a parametric description of the age distribution required in some other photometric methods.

4. TAURUS-AURIGA

As pointed out by Kenyon & Hartmann (1995, hereafter KH95), the Taurus-Auriga is an ideal laboratory to study low-mass star formation, since it is dominated by low-mass stars with little extinction, and so has been the subject of many investigations. The list of known members of the region has grown through the years (Cohen & Kuhl 1979; Herbig & Bell 1988, 1995; KH95; Briceño et al. 2002; Luhman 2004; Luhman et al. 2006; Guieu et al. 2006; Scelsi et al. 2007), with an increasing emphasis towards completeness.

As we discussed above, to estimate masses the XDPV method requires age estimates in addition to near-infrared photometry. We will take this age from the histogram of ages presented by KH95 (their Figure 16). They have derived these ages together with masses from a full set of visible and infrared photometry and spectral types for known Taurus-Auriga members. Their age distribution spans from $\log(\text{age}(\text{yr})) \equiv \log T = 4$ to 6.5 and we calculate a mean value of 5.95 and a median value of 5.8 ($T = 6.3 \times 10^5$ yr), which is smaller than the commonly assumed value of 6.3, and also smaller than the mean. We may then compare masses derived by our method. KH97 present spectral types and effective temperatures for 139 stars. They use 103 of them to construct a mass histogram from H-R diagrams with D’Antona & Mazzitelli (1994) tracks and CMA opacities. We took 189 stars with *JHK* photometry from their list, and calculated masses as described in § 2 above, using the median age derived ($\log T = 5.8$) from KH95, and the evolutionary models of D’Antona & Mazzitelli (1997) and <http://www.mporzio.astro.it/~dantona/prems.html>.

We compare mass histograms in Figure 2. To do so, we have re-binned KH95’s histogram in logarithmic 0.3 dex bins, by assigning random masses to each star within its own bin, and then re-binning in the logarithmic bins. We repeated this process 100 times to produce the mean histogram that is shown by dotted lines in Figure 2, while our mass histogram is shown as solid lines. For reference the Miller-Scalo IMF (Miller & Scalo 1979) is shown as a dashed line. The general shape from 0.3 to $1 M_{\odot}$ is remarkably similar in both histograms and both peak at the same value where a turnover is observed. The excess number of stars in our analysis (189 of 103) appear in three regions of the distribution. Some are in equal

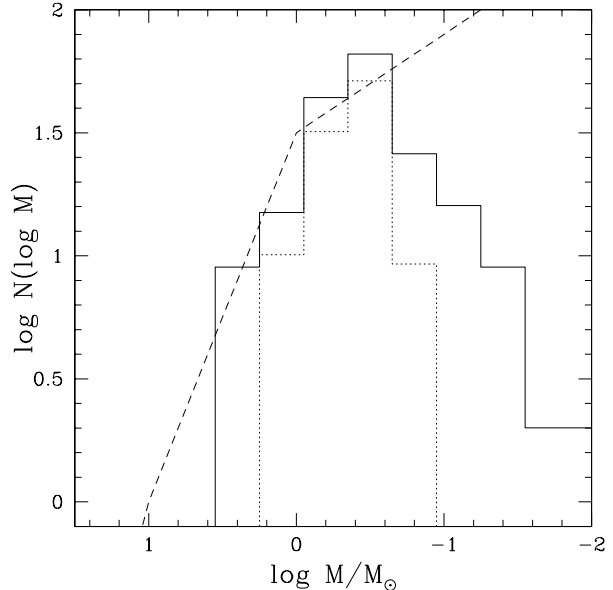


Fig. 2. IMF in Taurus-Auriga from Kenyon & Hartmann (1995) data processed by the XDPV method (shown as solid lines) compared to Kenyon & Hartmann (1995) mass histograms (dotted lines).

proportions in the three bins from $\log M = 0.1$ to $-0.5 M_{\odot}$, some lie in the high-mass end of the distribution, which nevertheless agrees quite well with the IMF of Miller & Scalo (1979), and the majority are distributed in low-mass bins $\log M/M_{\odot} < -0.8$, that most probably were too faint to provide a reliable spectral type by KH95. However, this low-mass region is not unbiased or complete, as is pointed out in their paper.

Briceño et al. (2002); Luhman (2004); Luhman et al. (2006) have paid attention to this fact, and have conducted spectroscopic surveys of several regions in the Taurus-Auriga clouds in order to identify all low-mass stars (many of which are brown dwarfs) to get complete unbiased samples of the IMF. This IMF is the result of photometry and spectroscopy to determine luminosities and effective temperatures, complemented with Baraffe et al. (1998) evolutionary tracks to derive masses. The more consolidated example of this IMF is given in Luhman (2004). We have taken the 2-MASS *JHK* data given in Luhman et al. (2006) for one of such complete regions that are consistent with Luhman (2004) IMF. In this new article, Luhman incorporated some 20 newly discovered brown dwarfs into a large region that encompasses about half of the known Taurus population, and thus constitutes a significant sample. With our method we were able to obtain solutions for 125 ob-

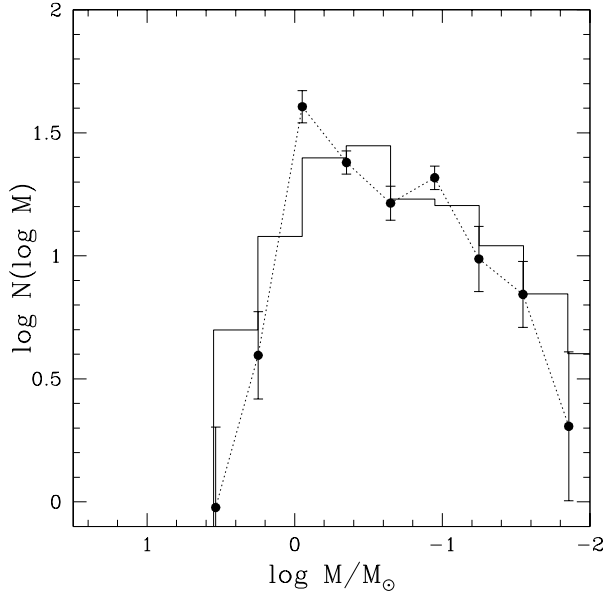


Fig. 3. IMF in Taurus-Auriga from Luhman et al. (2006) data as obtained by the XDPV method (shown as solid lines) compared to Luhman (2004)’s IMF (dotted lines).

jects out of the presented list of 156, again using the median age derived from KH95, and the evolutionary models of D’Antona & Mazzitelli (1997) and <http://www.mporzio.astro.it/~dantona/prems.html>.

As can be observed in Figure 3 the resemblance between the IMF obtained by Luhman (2004) and the IMF obtained using the XDPV method for the Taurus-Auriga region is remarkable, with a probability of over 60% of their being random samples of the same population. For a Kolmogorov-Smirnov test of this result and others, see § 6.

Furthermore, the XDPV solutions for both data sets (KH95; Luhman 2004) presented in Figures 2 and 3, resemble one another better than those presented in the original papers. We conclude that this agreement strengthens our results.

5. ORION NEBULA CLUSTER

5.1. About the IMF

The Orion Nebula Cluster (ONC) centered on the Trapezium OB stars is the richest of any nearby clusters and has been studied extensively. Numerous studies have targeted this cluster to determine its underlying population and the associated IMF (e.g., Hillenbrand 1997; Luhman et al. 2000; Muench et al. 2002). We will compare our own results to those of two important studies, one spectroscopic and one based on near-infrared photometry.

Hillenbrand (1997) has obtained spectral types for 934 visible stars. This information, supplemented

by optical photometry, allowed her to populate an H-R diagram with pre-main sequence evolutionary tracks, and to extract mass and age information. She notes, however, that large uncertainties arise from the choice of a particular set of evolutionary tracks (see also Hillenbrand & White 2004). Nevertheless, Hillenbrand (1997) chooses D’Antona & Mazzitelli (1994) evolutionary models to display the ONC’s IMF (her Figura 17), and it has become a seminal reference for this region. The derived distribution of stellar ages of the ONC population spans a wide range of ages. It starts at $\log T = 3.5$ (3000 yr) and increases gradually until $\log T = 6.3$ (2 Myr), then decreases abruptly and continues at a low constant pace up to $\log T = 7.8$ (63 Myr). This distribution has a mean value of $\log \langle T \rangle = 5.84$ (0.7 Myr) although some authors quote 0.8 Myr. It has also been represented by a constant rate from $\log T = 5$ (0.1 Myr) to $\log T = 6$ (1 Myr). In our treatment of the OMC cluster we will choose the median age, $\log T = 5.6$ (0.4 Myr), which we believe is the best compromise as is discussed above for Taurus-Auriga. This is in agreement with Luhman et al. (2000) work that also quotes a median age of 0.4 Myr.

Muench, Lada, & Lada (2000) developed a Monte Carlo method to model the IMF based on obtaining the KLF from a series of probability distributions: extinction, infrared excess, age and the IMF modeled as a series of power laws. They applied this method to *JHK* observations of the ONC in Muench et al. (2002). The age distribution was chosen as a uniform distribution from 0.2×10^6 to 1.4×10^6 yr. The extinction distribution was derived from a $(J - H)$ vs. $(H - K)$ diagram by de-reddening sources down to the classical T Tauri star locus of Meyer et al. (1997). After this, the infrared excess distribution was obtained from the remaining excess in the $(H - K)$ color after subtracting a histogram of $(H - K)$ colors of field stars, and this excess color was assumed to arise exclusively from excess disk emission at K . From an original set of ~ 1000 sources, they took an extinction limited sample ($A_V < 17$) of 583 stars, which is said to be complete down to $0.017 M_\odot$.

We took *JHK* photometry from the Muench et al. (2002) published list, assumed a median age of $\log T = 5.6$ from the Hillenbrand (1997) age histogram, used the D’Antona & Mazzitelli (1997) and <http://www.mporzio.astro.it/~dantona/prems.html> evolutionary tracks, and assumed a distance of 400 pc (Muench et al. 2002). With these ingredients we applied our XDPV method to the 699 object for which no confusion flags

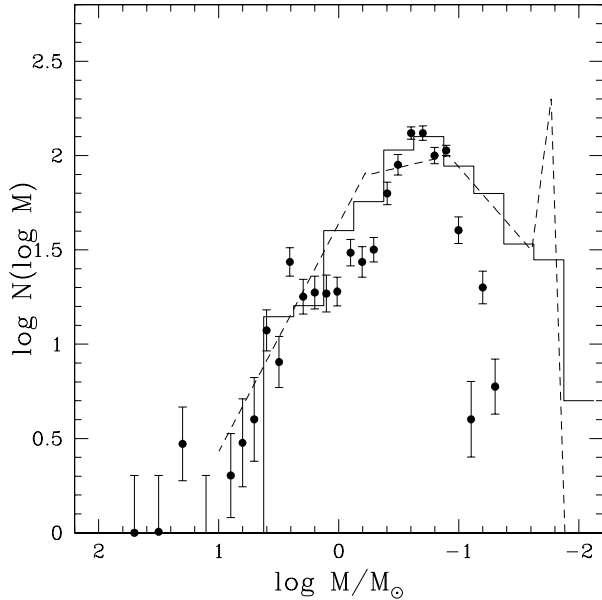


Fig. 4. ONC’s IMF (solid histogram) compared to Hillenbrand (1997) (points with error bars) and Muench et al. (2002) (dashed line).

are found and photometry is available in all *JHK* filters. We were able to obtain solutions consistent with both $\alpha > 0$ and $\beta > 0$ and an acceptable $\text{Err} < 0.3$ mag for 612 of these stars. Objects for which no solution was found are, for example, stars more massive than those present in the D’Antona & Mazzitelli (1997) and <http://www.mporzio.astro.it/~dantona/prems.html> evolutionary tracks, maximum of $3 M_{\odot}$, which includes all the Trapezium stars, BN and $\Theta^2\text{Ori A}$. From the 612 PMS objects we then selected 578 with $A_V < 17$ to display in Figure 4. This compares our IMF (solid histogram) with that of Hillenbrand (1997), shown as points with error bars, and Muench et al. (2002), shown as a dashed line. The agreement with Muench et al. (2002) is excellent, that is, the initial slope for high-mass stars, the flattening and the position of the turnover, followed by the negative slope in the subsolar mass spectrum all agree quite well. The only exception is for the low-mass secondary peak in the substellar region ($\log M/M_{\odot} = -1.8$). Unfortunately, those objects come from the low-brightness peaks in the *H* and *K* histograms in Muench et al. (2002) but are too faint and red, and therefore, absent in *J*. Consequently, they do not appear in our data.

The agreement with the Hillenbrand (1997) IMF is quite good in the $-0.9 < \log M/M_{\odot} < 0.45$ range. Massive stars ($M > 3 M_{\odot}$) are missing in

our histogram as mentioned above, due to the limited mass range in the evolutionary tracks. In the $\log(M/M_{\odot}) < -1$ range, the Hillenbrand (1997) survey is most likely incomplete for sources with $A_V > 2.5$ (Hillenbrand & Carpenter 2000). The position of the turnover also agrees, although the exact position may be at slightly lower masses as has been revised in Hillenbrand & Carpenter (2000) by using updated evolutionary tracks and transformations.

We conclude that the IMF we obtained with the XDPV method is a robust representation of that obtained by other methods. For a more thorough comparison of these distributions see § 6.

5.2. Extinction and infrared excess

In addition to the mass data, our method also gives information about the extinction α and infrared excess β of the sources. We display these two quantities as histograms in Figure 5, and compare them with extinctions and excesses used in Muench et al. (2002) and Hillenbrand (1997).

The bottom left panel shows the histogram of extinction α as a solid histogram. This quantity can be directly understood in terms of the visual extinction, $\alpha = A_V/10$. It is then easy to compare it with the extinction probability distribution presented in Muench et al. (2002), shown here as a solid line, which is very close to our result. In order to compare with the spectroscopically derived extinctions in Hillenbrand (1997), we show the dashed histogram for those sources that were analyzed by us and that are also part of the Hillenbrand (1997) survey, and compare it to the dashed line obtained from extinctions derived by her. A discrepancy is notorious for the very low extinction ($A_V < 2$) sources, where Hillenbrand (1997) finds most sources and our histogram turns over.

In the bottom right panel we show the histogram for β compared to the infrared excess distribution in Muench et al. (2002). However, there are two possibilities for this comparison. If the abscissa in Muench et al. (2002, Figure 8b) is the excess in $H - K$, then from equation (2) $\beta = E_{H-K}/(y_K - y_H)$, while if the abscissa is taken as the excess in *K* alone, then $\beta = -E_K/y_K$, and given the values in Table 1, they are not equal. We show both possibilities in Figure 5d. The infrared excess is best represented by β and we find a better agreement when the infrared excess distribution is represented by $-E_K$, rather than E_{H-K} .

In the top panels of Figure 5 we show α and β as functions of mass $\log M$. As a general rule, no dependence of these two quantities with mass is found,

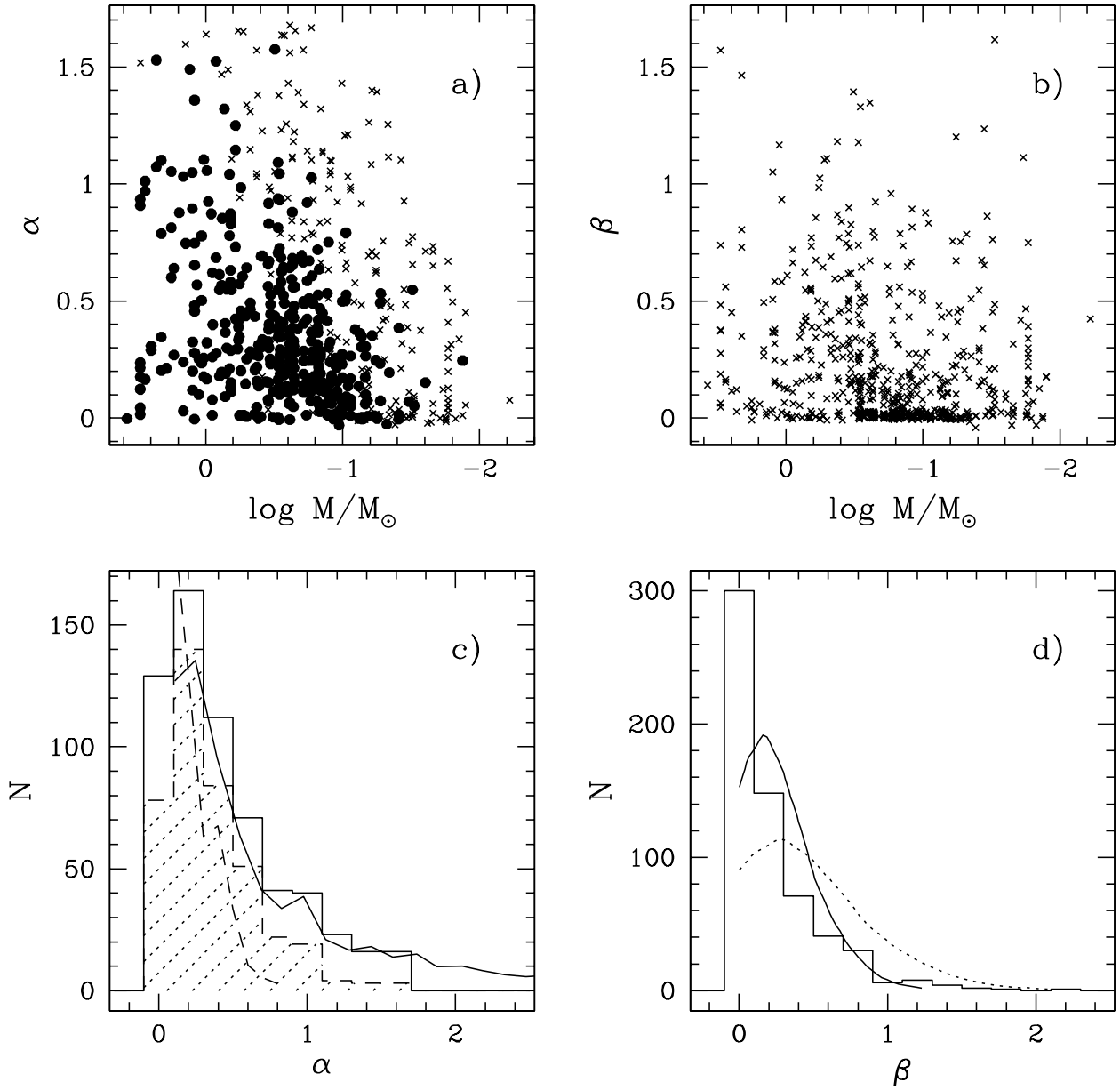


Fig. 5. Top panels: α and β as function of mass. In panel (a) sources also in the survey of Hillenbrand (1997) are marked as dots. Bottom panels: histograms of α and β in solid lines, are compared to (c) the extinction probability distribution of Muench et al. (2002) solid line, and the extinction data in Hillenbrand (1997) in dashed line to its corresponding dashed line histogram. (d) The infrared excess probability distribution of Muench et al. (2002) if considered as $E(H - K)$ (dashed line) or K -excess (solid line).

as α and β acquire all their values for any mass in the range from 0.017 to $3.0 M_{\odot}$. The one exception is observed in the case of α (Figure 5a): there are no low-mass stars at high extinctions. This is more evident in the case of those stars also observed by Hillenbrand (1997), marked as solid dots, where a diagonal line in the uppermost right part of the diagram

can easily be drawn. This is expected to be the case, since low-mass stars cannot be observed at high extinctions for given observation times; and since this fact was not introduced a priori in the method, it constitutes another confirming result of the XDPV approach. In this diagram it is then possible to extract an extinction limited sample, as a rectangular

box that lies below the diagonal line corresponding to each sample. It can be seen that the Hillenbrand (1997) survey is unbiased for $\log M/M_{\odot} > -1.1$ and $A_V < 3$, in close agreement with her findings (see also Hillenbrand & Carpenter 2000). On the other hand, the completeness limit in all three *JHK* filters in the Muench et al. (2002) survey would go up to $\log M/M_{\odot} > -1.8$ and $A_V < 6$. Finally, given that the infrared excess β is due to the disk contribution we find that 300 stars out of 612 (close to 50%) presumably possess associated disks ($\beta > 0$), independently of their mass. This is consistent with recent Spitzer studies that show that the percentage of low-mass PMS stars with disk in ONC is about 50% (Rebull et al. 2006; Cieza & Baliber 2007).

6. STATISTICAL SIGNIFICANCE OF IMFS

For two young stellar clusters a general concern is whether the individual IMFs are different or not, given that the shapes of the IMFs look similar. To quantify this we performed a Kolmogorov-Smirnov (K-S) test. First, we compared the most accepted mass distributions for Taurus and Orion, to show that they are significantly different. Second, we compared the IMFs obtained by the XDPV method to both the Taurus and Orion cases.

To perform the K-S test we developed a routine that generates a random population of stellar masses from any given mass distribution $N(\log M)$ using the well known accept-reject algorithm. For each distribution that we tested, we generated a number of random stellar masses equal to the number of stars that were used to obtain the original distribution, in order to keep the same stochastic variability that would be expected in a different realization of the distribution. For each comparison between different distributions, we took 100 realizations of each distribution being compared, and computed the two distribution K-S probabilities that the samples are drawn from the same parent distributions (null hypothesis). We report the mean of these 100 comparisons (K-S MP).

We first tested the IMFs reported by Luhman (2004) for Taurus-Auriga (hereafter TL) and compared it with those of Hillenbrand (1997) and Muench et al. (2002), hereafter OH and OM respectively, for Orion. The OH distribution has the advantage of being derived spectroscopically (as well as the TL one), but is incomplete for masses lower than $\log(M/M_{\odot}) < -0.9$ as we already mentioned. For this reason we limited this distribution to the medium mass range in the comparisons. We therefore label it as OHM. Similarly, as we already discussed, the OM distribution has a secondary peak at

the very low mass end which we cannot test because the sources involved are below the J filter detection limit. Therefore the OM distribution is limited to $\log(M/M_{\odot}) > -1.6$ for all tests here. The comparisons between TL and OHM yield a K-S mean probability (K-S MP) of 3×10^{-11} of being drawn from the same parent distribution, while TL and OM gives K-S MP of 1×10^{-4} . These very small values make us confident that our test is consistent with previously known results (e.g., Lada et al. 2008) that the distributions are indeed different.

We then compared the distribution of XDPV masses obtained for the Taurus-Auriga region (hereafter TX) to TL, obtaining a K-S MP of 21% therefore confirming the possibility of both distributions being equivalent representations. The comparison of TX to OHM rules out the null hypothesis with a K-S MP of 6×10^{-5} . It should be mentioned however, that TX is not that different from OM (K-S MP of 1%) mainly because in the low mass range $-1.6 < \log(M/M_{\odot}) < -0.9$ TL is quite similar to OM (K-S MP = 67%). That is to say, the low mass slope of Taurus and Orion IMFs are similar. Nevertheless, the agreement between TX and TL is sustained.

Finally, the distribution of XDPV masses obtained for the Orion region (hereafter OX) compares with OHM with a K-S MP of 3% in the medium mass range, and a somewhat better agreement is seen to OM with K-S MP = 9% in the whole range of masses $\log(M/M_{\odot}) > -1.6$. On the other hand, OX and TL cannot be accepted as a match with a very low K-S MP of 2×10^{-7} . This proves that OX is not consistent with the Taurus IMF but has a fair probability of being drawn from the same parent population of the Orion Nebula Cluster.

7. SUMMARY

We used the extinction-disk-principal vectors approach, which is called the XDPV method, reported previously in LS07, to show that it is a powerful tool to estimate masses of pre-main sequence stars in clusters. The method requires a minimum of information, using as little as *JHK* (or *IJK* or *JKL*) near-infrared photometry, supplemented by a set of PMS evolutionary tracks (e.g., D'Antona & Mazzitelli 1997) and the median age of the cluster. For each star in the cluster we are able to estimate the contribution of the extinction vectors \vec{X}_{cc} in the color-color diagram and \vec{X}_{cm} in the color-magnitude diagram, and the disk vectors \vec{D}_{cc} in the color-color diagram and \vec{D}_{cm} in the color-magnitude diagram, using D'Alessio et al. (2005) accretion disk model

grids of spectral energy distributions. The observed absolute magnitude at each wavelength λ of a PMS object is obtained via $m_\lambda = m_\lambda^0(\text{mass, age}) + d + \alpha x_\lambda - \beta y_\lambda$, where the first term corresponds to the absolute magnitude of the naked object for a certain mass and age, followed by the distance modulus d , the extinction correction (αx_λ) and the infrared excess contribution ($-\beta y_\lambda$) from the circumstellar disk. It is shown that if a representative age of the cluster, such as the median, is known, the masses of each individual star can be statistically obtained from its near-infrared photometry alone. The XDPV method is tested in the well studied regions of Taurus-Auriga and the Orion Nebula Cluster by extracting their Initial Mass Function. These IMF are in excellent agreement (K-S test) to those given by KH95 and Luhman (2004) for Taurus and Hillenbrand (1997) and Muench et al. (2002) for Orion. Since our algorithm also yields the extinction and disk contribution for each star, the distributions can be obtained. The overall extinction distribution for the Orion cluster is analyzed and compares well with previous work; the comparison to Muench et al. (2002) shows that the parameter α for the extinction vector is $-E_K$ rather than E_{H-K} . The frequency of PMS low-mass stars with disks, represented by the parameter β , is about 50% in the Orion sample. It is also seen that the number of sources observed decreases for high values of extinction α , confirming a well known and expected observational effect, and allowing us to draw a complete extinction limited sample a posteriori. We conclude that our XDPV algorithm can be applied to study the IMF of young stellar clusters, as well as the distributions of extinction and disk infrared excess.

We are grateful to an anonymous referee for very valuable comments that aided in the final version of the manuscript.

REFERENCES

- Baraffe, I., Chabrier, G., Allard, F., & Hauschildt, P. H. 1998, *A&A*, 337, 403
- Briceño, C., Luhman, K. L., Hartmann, L., Stauffer, J. R., & Kirkpatrick, J. D. 2002, *ApJ*, 580, 317
- Cieza, L., & Baliber, N. 2007, *ApJ*, 671, 605
- Cohen, M., & Kuhi, L. V. 1979, *ApJS*, 41, 743
- D'Alessio, P., Merín, B., Calvet, N., Hartmann, L., & Montesinos, B. 2005, *RevMexAA*, 41, 61
- D'Antona, F., & Mazzitelli, I. 1994, *ApJS*, 90, 467
- . 1997, *Mem. Soc. Astron. Italiana*, 68, 807
- Guieu, S., Dougados, C., Monin, J.-L., Magnier, E., & Martín, E. L. 2006, *A&A*, 446, 485
- Herbig, G. H., & Bell, K. R. 1988, *Third Catalog of Emission Line Stars of the Orion Population (Santa Cruz: Lick Obs.)*
- . 1995, *VizieR Online Data Catalog*, 5073, 0
- Hillenbrand, L. A. 1997, *AJ*, 113, 1733
- Hillenbrand, L. A., & Carpenter, J. M. 2000, *ApJ*, 540, 236
- Hillenbrand, L. A., Strom, S. E., Vrba, F. J., & Keene, J. 1992, *ApJ*, 397, 613
- Hillenbrand, L. A., & White, R. J. 2004, *ApJ*, 604, 741
- Kenyon, S. J., & Hartmann, L. 1995, *ApJS*, 101, 117 (KH95)
- Lada, C. J., & Adams, F. C. 1992, *ApJS*, 393, 278
- Lada, C. J., Muench, A. A., Rathborne, J., Alves, J. D., & Lombardi, M. 2008, *ApJ*, 672, 410
- López-Chico, T., & Salas, L. 2007, *RevMexAA*, 43, 15 (LS07)
- Luhman, K. L. 2004, *ApJ*, 617, 1216
- Luhman, K. L., Lada, E. A., Muench, A. A., & Elston, R. J. 2005, *ApJ*, 618, 810
- Luhman, K. L., Whitney, B. A., Meade, M. R., Babler, B. L., Indebetouw, R., Bracker, S., & Churchwell, E. B. 2006, *ApJ*, 647, 1180
- Luhman, K. L., et al. 2000, *ApJ*, 540, 1016
- Meyer, M. R., Calvet, N., & Hillenbrand, L. A. 1997, *AJ*, 114, 288
- Miller, G. E., & Scalo, J. M. 1979, *ApJS*, 41, 513
- Muench, A. A., Lada, E. A., & Lada, C. J. 2000, *ApJ*, 533, 358
- Muench, A. A., Lada, E. A., Lada, C. J., & Alves, J. 2002, *ApJ*, 573, 366
- Palla, F., & Stahler, S. W. 1999, *ApJ*, 525, 772
- Rebull, L. M., Stauffer, J. R., Megeath, S. T., Hora, J. L., & Hartmann, L. 2006, *ApJ*, 646, 297
- Rieke, G. H., & Lebofsky, M. J. 1985, *ApJ*, 288, 618
- Scelsi, L., et al. 2007, *A&A*, 468, 405

Irene Cruz-González: Instituto de Astronomía, Universidad Nacional Autónoma de México, Apdo. Postal 70-264, 04510 México D. F., Mexico (irene@astrocu.unam.mx).

Luis Salas: Instituto de Astronomía, Universidad Nacional Autónoma de México, Apdo. Postal 877, 22830, Ensenada, B. C., Mexico (salas@astrosen.unam.mx).